

INSTABILITY OF STATIONARY AND UNIFORMLY MOVING CYLINDRICAL FLUID BODIES—II

VISCOELASTIC THREADS AND EXPERIMENTAL OBSERVATIONS

WEI-KUO LEE†, KUO-LIANG YU and RAYMOND W. FLUMERFELT

Department of Chemical Engineering, University of Houston, Houston, TX 77004, U.S.A.

(Received 27 April 1980; in revised form 16 October 1980)

Abstract—The instability analysis of Part I is extended to the breakup of viscoelastic threads in fluid media (also possibly viscoelastic). Critical Growth rates and wave-numbers are calculated in terms of the viscosity ratio, the Ohnesorge numbers (continuous and dispersed phases), and elasticity numbers for each of the respective phases. Comparisons with results for Newtonian systems indicate viscoelastic threads to be less stable than Newtonian threads under similar conditions. Also, the critical wave-numbers observed with viscoelastic threads can differ significantly from those observed with Newtonian systems, particularly if the relative magnitudes of elasticity of the dispersed and continuous phases are quite different. Systems with similar magnitudes of elasticity in each phase exhibit wave-numbers similar to Newtonian systems of similar viscosities.

Experimental results obtained from observations of fluid thread breakup in a Taylor four-roller device provide a basis for checking the predictions of the linearized theory for both Newtonian and viscoelastic systems. In general, the agreement is good and the theoretical predictions of Parts I and II seem to be reasonable representations of experimental fact.

INTRODUCTION

The instability of stationary cylindrical bodies of Newtonian fluids has been analyzed in Part I of this paper. The corresponding problem for non-Newtonian viscoelastic fluids is considered here as well as the comparison of the predictions with experimental observations on both Newtonian and non-Newtonian systems obtained with a Taylor four-roller apparatus.

Previous work on the instability of viscoelastic cylindrical fluid bodies has been mainly concerned with the breakup of laminar jets in inviscid fluids. Middleman (1965) first analyzed this problem assuming that the viscoelastic jet was that of a linearized Oldroyd fluid. He showed that a viscoelastic jet will be less stable than a Newtonian jet, under identical dynamic conditions. Supporting experimental results with slightly "elastic" polymer fluids were obtained later by Krosser and Middleman (1969). Golden *et al.* (1969) analyzed this problem using a general linear viscoelastic constitutive equation and expressed their results in terms of the complex viscosity function. Like Middleman, these investigators derived a characteristic equation for the disturbance growth rate analogous to Weber's equation for Newtonian fluids; the only difference being that the Newtonian viscosity was replaced by the complex viscosity function. The results of this linear analysis also showed the viscoelastic jet to be less stable than the Newtonian jet. In the same paper, these investigators also reported experimental data on the breakup of Newtonian, inelastic non-Newtonian, and viscoelastic jets; a later paper by Golden *et al.* (1972) reported data on jets of inelastic non-Newtonian fluids with yield stresses. The inelastic non-Newtonian fluid jets exhibited instabilities similar to Newtonian jets when the viscosities corresponded to the structurally degraded non-Newtonian fluid exiting from the capillary tube. The viscoelastic jets exhibited breakup patterns quite different from the observations with the Newtonian and non-Newtonian inelastic jets. In particular, no discernible wave formation was evident and the first visible disturbances appeared as large droplets, randomly distributed and connected by smaller diameter continually thinning threads. The first

†Present address: Exxon Research and Engineering Co., Linden, NJ 07036, U.S.A.

appearance of these droplets occurred at "breakup" lengths shorter than those obtained for Newtonian systems with comparable zero-shear viscosities. The final breakup lengths of the beaded threads, however, were found to be significantly higher than those for similar Newtonian jets.

Obviously, the irregular breakup patterns observed with viscoelastic jets do not correspond to the predicted disturbance growth patterns of the linearized analysis, even qualitatively. This does not infer, necessarily, that the linear analysis is invalid for describing observable breakup phenomena of stationary or uniformly moving viscoelastic threads. Instead, it may be argued that a viscoelastic jet does not represent a truly relaxed, stationary thread. In particular, because of shear in the tube nozzle, the jet may experience stress relaxation over a jet length comparable to the breakup length, or even greater. Under such conditions, the breakup behavior could deviate markedly from that of a relaxed stationary thread. Moreover, a beaded thread is well-deformed as compared to that considered in the linearized theory. Because of these effects, the breakup of viscoelastic capillary jets does not represent a particularly useful experiment in testing the validity of the linearized analysis. It would appear that some of the experiments first proposed by Taylor (1934) for studying drop extension and thread breakup in immiscible systems are more meaningful in this regard.

In the present paper, we use the methods of linearized stability theory to analyze the instability of a stationary viscoelastic thread in another medium, also possibly viscoelastic. Linear viscoelasticity is assumed to hold and the results are expressed in terms of the complex viscosity functions of each phase. The results of Middleman (1965) and Golden *et al.* (1969) arise as special cases of the analysis, just as Weber's equation arises as a special case of stationary Newtonian thread problem. The theoretical predictions of the analysis are checked with experimental data on stationary thread breakup in a Taylor four-roller apparatus. Data are provided for both Newtonian and viscoelastic systems which cover a wide range of dispersed phase and continuous phase material behavior. In general, the results provide various insights into the mechanics of the breakup process, the roles of the physical forces, and the validity of the linearized theory. It is useful in understanding not only the breakup of jets, but also more generally, the breakup of fluid threads in fluid media.

SMALL DEFORMATION FLOWS OF VISCOELASTIC FLUIDS

The behavior of viscoelastic fluids in small deformation flows is describable within the framework of linear viscoelasticity. The constitutive relation appropriate to such behavior is given by (Bird *et al.* 1977):

$$\tau = - \int_{-\infty}^t \Phi(t-t') \dot{\gamma}(t') dt' \quad [1]$$

which specifies the stress field τ at time t as an integral of the current and past values of the strain rate $\dot{\gamma}$. The quantity $\Phi(t-t')$ is the relaxation modulus which appropriately weights the strain rate effects of previous history. Equation [1] is often referred to as the Boltzmann equation for linear viscoelastic behavior. In the case of Newtonian fluids, $\Phi = \eta \delta(t)$, where $\delta(t)$ is the Dirac δ function and τ depends only on the instantaneous value of $\dot{\gamma}$ at the moment $t' = t$.

Here we consider a class of oscillatory flows for which the strain rate and stress fields are described by

$$\dot{\gamma} = \text{Re}\{\dot{\gamma}^* e^{i\omega t}\} \quad [2]$$

$$\tau = \text{Re}\{\tau^* e^{i\omega t}\} \quad [3]$$

where ω is the frequency of the oscillation, and $\text{Re}\{ \}$ denotes the real part of the complex quantity $\{ \}$. The quantities $\dot{\gamma}^*$ and $\dot{\tau}^*$ are complex strain rate and stress amplitudes.

Substituting these expressions for τ and $\dot{\gamma}$ into the Boltzmann equation [1] we find

$$\tau^* = -\eta^* \dot{\gamma}^* \tag{4}$$

where η^* is the complex viscosity function defined by

$$\eta^* = \int_0^\infty \Phi(s) e^{-i\omega s} ds \tag{5}$$

and $s = t - t'$. Hence the complex viscosity function represents a one-sided Laplace transform of the relaxation function, i.e. $\bar{\Phi}(i\omega)$.

Based upon extensions of the simple single element Maxwell model to multiple elements it is possible to obtain the following form for Φ corresponding to the generalized Maxwell model (Bird *et al.* 1977, pp. 278–279):

$$\Phi(s) = \sum_{q=1}^\infty [(\eta_q e^{-s/\Lambda_q})/\Lambda_q] \tag{6}$$

where η_q and Λ_q are the viscosities and time constants of the individual viscoelastic elements, respectively. From molecular theory results of Rouse and empirical observations, Spriggs (1965) proposed the following simplifications:†

$$\eta_q = \eta_0 \frac{\Lambda_q}{\sum_{q=1}^\infty \Lambda_q} = \frac{\eta_0}{q^\kappa Z(\kappa)} \tag{7}$$

$$\Lambda_q = \frac{\Lambda}{q^\kappa} \tag{8}$$

where $Z(\kappa) = \sum_{q=1}^\infty q^{-\kappa}$ denotes the Riemann–Zeta function. We then have

$$\eta^* = \frac{\eta_0}{Z(\kappa)} \left[\sum_{q=1}^\infty \left(\frac{q^\kappa - i\omega\Lambda}{q^{2\kappa} + (\omega\Lambda)^2} \right) \right] \tag{9}$$

or, replacing $(i\omega)$ by ϵ

$$\eta^* = \bar{\Phi}(\epsilon) = \frac{\eta_0}{Z(\kappa)} \left[\sum_{q=1}^\infty \left(\frac{1}{q^\kappa + \alpha\Lambda} \right) \right]. \tag{10}$$

Hence the fluid behavior for small amplitude oscillatory motions can be obtained from [2] to [4] and [10] by specifying three material parameters: the zero-shear viscosity η_0 , a time constant Λ , and a slope parameter κ in the power-law region. Such a description has been found to describe the experimentally observed behavior of viscoelastic fluids undergoing small amplitude oscillatory flows in viscometric instruments (Huppler *et al.* 1967).

THE INSTABILITY OF LIQUID THREADS IN VISCOELASTIC SYSTEMS

By taking a two-sided Laplace transform of the linearized equations of motion, we obtain

$$-\rho\epsilon\hat{\underline{u}} = \nabla\hat{p} + \nabla\cdot\hat{\underline{\tau}} = \nabla\hat{p} + \hat{\eta}(\epsilon)[\nabla\cdot\hat{\underline{\gamma}}] \tag{11}$$

†Here, the Weissenberg hypothesis is considered to eliminate an additional parameter, the shift factor, in Spriggs model.

where the terms with a “ \wedge ” are the transformed quantities defined by

$$\hat{\Psi}(\epsilon) = \int_{-\infty}^{\infty} \Psi(t) e^{-\epsilon t} dt. \quad [12]$$

The quantity $\hat{\eta}(\epsilon)$ is equivalent to $\eta^*(\epsilon)$, the complex viscosity function at the frequency ϵ , i.e. $\hat{\eta}(\epsilon) = \bar{\Phi}(\epsilon) = \eta^*(\epsilon)$. We also can take the two-sided Laplace transform of the equation of continuity, and by introducing the Stokes' stream function, obtain the velocity components:

$$\hat{u}_r = \frac{1}{r} \frac{\partial \hat{\psi}}{\partial z}, \quad \hat{u}_z = -\frac{1}{r} \frac{\partial \hat{\psi}}{\partial r}. \quad [13]$$

From this point the analysis follows the same procedure as presented in the preceding paper on Newtonian systems. By replacing u by \hat{u} , ψ by $\hat{\psi}$, η by $\hat{\eta}$, U by η_D/η_C , etc. an identical form of [10] in the preceding paper (Part I) can be obtained.

In Newtonian systems $\hat{\eta} = \eta$, and mathematically we have the Newtonian problems described previously. In non-Newtonian viscoelastic systems, the problem is somewhat different since $\hat{\eta}$ is a function of ϵ , the frequency of the disturbance wave on the thread. Hence, the instability problem depends not only on the physical properties of the fluid systems involved, but also on the kinematic conditions of the disturbance waves.

To close the problem, a suitable rheological constitutive equation is required. Since we are dealing with small disturbances where linearized stability analysis is valid, the motions are assumed to be within the domain where linear viscoelasticity theory can be applied, i.e. small deformations. Thus, it is reasonable to use a constitutive equation based on linear viscoelasticity. Owing to the fact that it contains easily measurable parameters and accurately describes real material behavior, the relation given by [10] is used here.

Hence the problem consists of solving the individual motion equations for the thread and continuous phase and then coupling these results with the same boundary conditions as given in Part I. It should be noted that the results cover the full range of possibilities, i.e. Newtonian threads in Newtonian or viscoelastic continuous phase, and viscoelastic threads in Newtonian or viscoelastic continuous phase.

The dimensionless parameters in the problem can be summarized as (refer to the parallel relation in [10] of Part I): $U = (\hat{\eta}_D/\hat{\eta}_C)$; $G = (\rho_D/\rho_C)$; $S = (a\alpha\eta_{OC}/\sigma)$; $T_C = (\sigma\Lambda_C/2a\eta_{OC})$; $T_D = (\sigma\Lambda_D/2a\eta_{OD})$; $X = ka$: κ_D and κ_C . In order to simplify the problem, only the limiting case where $Oh_D \sim Oh_C \rightarrow 0$ is considered since the Ohnesorge number is usually very small in the case of liquid threads immersed in liquid media. We can also eliminate the density ratio, G , and discuss the problem with seven parameters if both the dispersed and the continuous phases are viscoelastic fluids.

The problem is then analogous to that described by [14] of Part I with U replaced by $U = \bar{\Phi}_D/\bar{\Phi}_C$. From [10] we can write

$$\bar{\Phi} = \frac{\eta_0}{Z(\kappa)} \left[\sum_{q=1}^{\infty} \left(\frac{1}{q^\kappa + \epsilon\Lambda} \right) \right] = \eta_0 \Phi^* \quad [14]$$

and

$$U = \frac{\eta_{OD}\Phi_D^*}{\eta_{OC}\Phi_C^*} = H \frac{\Phi_D^*}{\Phi_C^*} \quad [15]$$

where H is the ratio of zero-shear viscosities, η_{OD}/η_{OC} ; $\Phi^*(\epsilon)$ can be considered as a measure of the viscoelasticity; and U can be considered as the ratio of apparent viscosities. If either the

dispersed phase or the continuous phase is Newtonian, the corresponding Φ^* will reduce to unity.

Numerical results

The following numerical evaluations were made based on the analogy with [14] of Part I, but extended here to viscoelastic systems. Note that, in all cases, higher growth rates and more unstable systems are predicted for viscoelastic fluids.

Figure 1 shows the result for systems with equal viscosities. It can be seen that the (dimensionless) growth rate $S_{VD}(=S_{VC}$ here) increases with the increases of T_D and T_C . The results for Newtonian systems are given by the curves with $T_D = T_C = 0$. For viscoelastic systems, the values of S are always higher than the Newtonian cases. Moreover, it can be seen in figure 1(a) that X^* , the wavenumber corresponding to the maximum growth rate S^* , is the same in all cases of equal "elasticity" in both phases ($T_D = T_C, \kappa_D = \kappa_C$). This result will not be true when $T_D \neq T_C$ as shown in figure 1(b).

Figure 2 shows plots of the dimensionless critical growth rates and wave-numbers (S^* and X^*) for two systems with $H < 1.0$. The argument mentioned in the last paragraph is still true since vertical lines can be drawn at $X^* = 0.4134$ for $H = 0.01$ and 0.5677 for $H = 0.1$. When the magnitudes of elasticity are different in the two phases, a network of S^*-X^* plots show that the increase of elasticity of continuous phase increases the value of X^* , whereas the elasticity of dispersed phase shows an opposite effect. Since the wavenumber can be used to predict the size of broken droplets, the results for cases with equal elasticity in both phases imply that the ultimate drop size resulting from the breakup of a thread is independent of the absolute magnitude of the elastic effects in the phases. Moreover, the results in figure 2 also imply that the size of droplets can be altered by changing the relative magnitudes of the elasticity in the dispersed and the continuous phases. This could be an interesting result, particularly to those concerned with multiphase mixing and dispersion of viscoelastic systems. It should be noted that the bottom curves in figures 2(a) and 2(b) are for cases of Newtonian continuous phase ($T_C = 0$) or dispersed phase ($T_D = 0$) respectively; they are also the lower bounds of this network.

As for the results in cases where $H > 1$, figure 3 shows the results for systems with $H = 10$. The "elasticity" still increases the instability (or growth rate), but a different behavior is noted for the $H > 1$ case than for the previous $H < 1$ cases (figure 2). In particular, a reverse effect of

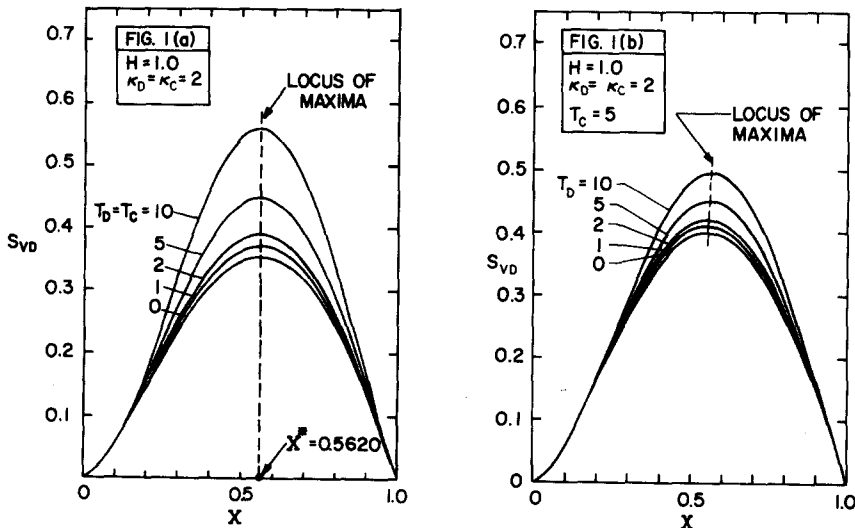


Figure 1. Dependence of disturbance growth rate on disturbance wave number; in viscoelastic systems ($T_D \geq 0, T_C \geq 0$) with $\eta_{0D} = \eta_{0C}$ (or $H = 1.0$).

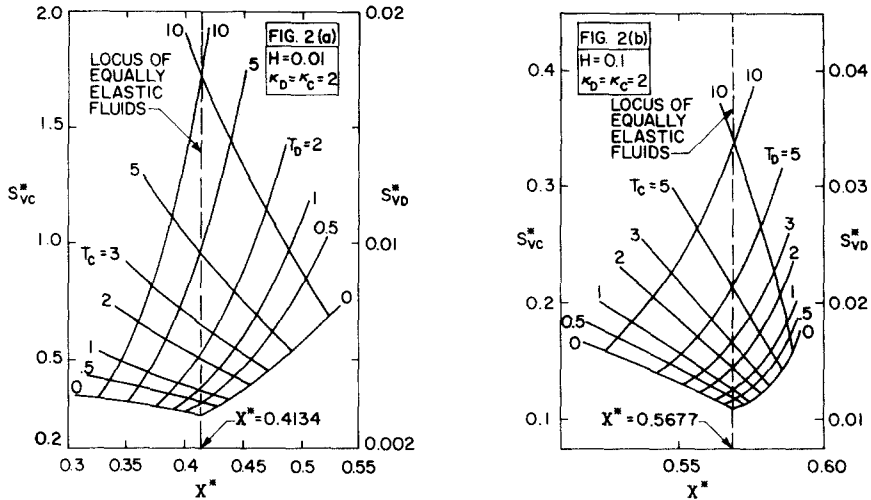


Figure 2. Effects of continuous and dispersed phase elasticity on the critical growth rate and critical wave number. (a) $H = \eta_{OD}/\eta_{OC} = 0.01$, and (b) $H = 0.1$.

the dispersed phase and continuous phase elasticities is obtained (compare the T_D , T_C lines of figures 2 and 3).

This result is more apparent in figure 4 which gives the dependence of X^* on H . In this figure it is clear that in systems where $\eta_{OD}/\eta_{OC} < 0.2$, an increase of "elasticity" in the continuous phase increases X^* and such an increase in the dispersed phase decreases X^* . A transition range is found around $H \sim 0.2$ and opposite effects arise for all system with higher viscosity ratios. We also find a wider range of X^* for viscoelastic systems where $H < 0.1$ than those where $H > 1$. In the latter cases, the elasticity effects on X^* are minor.

The above discussions are restricted to systems with κ_D and $\kappa_C = 2$. A study of the effects of κ on the instability problem can be found in figure 5. The increase in κ does increase the growth rate of unstable waves, however, the change is quite small, indicating that κ may be considered as a minor factor in the instability problem.

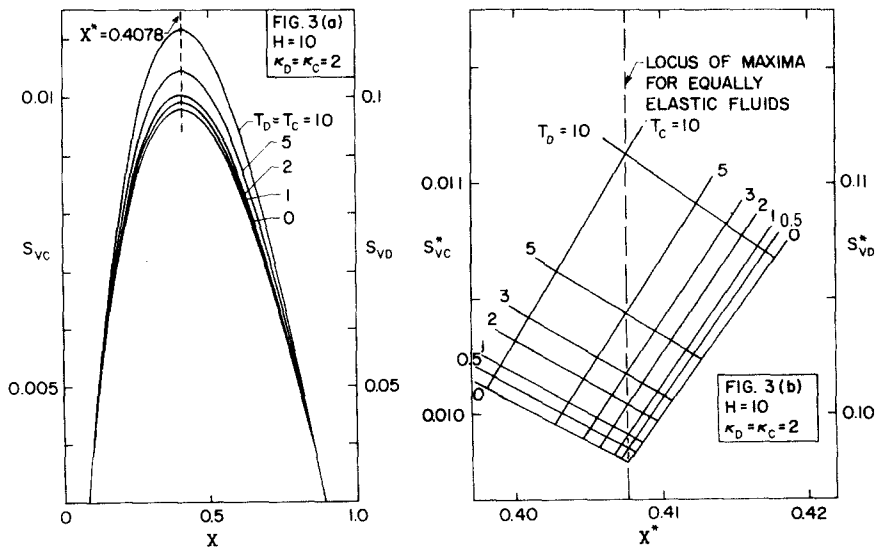


Figure 3. Effects of continuous and dispersed phase elasticity on critical growth rate and critical wave number. The dispersed phase is significantly more viscous than continuous phase ($H = 10$).

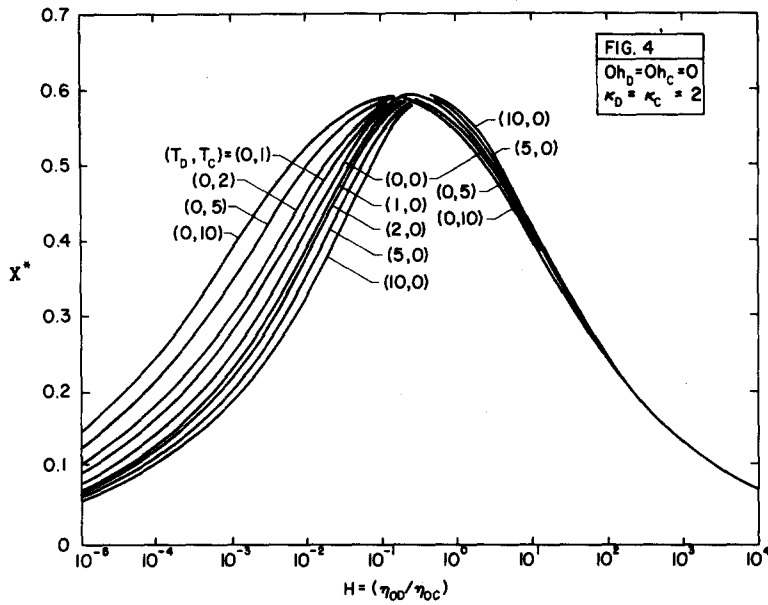


Figure 4. Dependence of critical wave number on elasticity numbers and viscosity ratio in systems with $Oh_C = Oh_D = 0$.

The two extreme cases corresponding to H approaching 0 and ∞ , respectively, are shown in figures 6 and 7, and are based on the corresponding limiting relations in [16] and [15] of Part I for viscoelastic media. These figures justify that the observations made by previous investigators that viscoelastic threads are less stable than Newtonian threads (all things being equal).

EXPERIMENTAL STUDIES

In his pioneering studies on the breakup of liquid drops in various flow fields, Taylor (1934) employed a four roller apparatus like shown in figure 8 to study breakup in plane hyperbolic flow fields. In this apparatus, the continuous phase flow field is set up through the motion of four cylinders (or rollers) located at the corners of a square or rectangle. The dispersed phase drop is placed at or near the stagnation point of the flow field (point O) and is maintained at this point through slight tandem control adjustments in the rotation speed of the left-and-right side roller pairs (see Lee 1972 and Yu 1974).

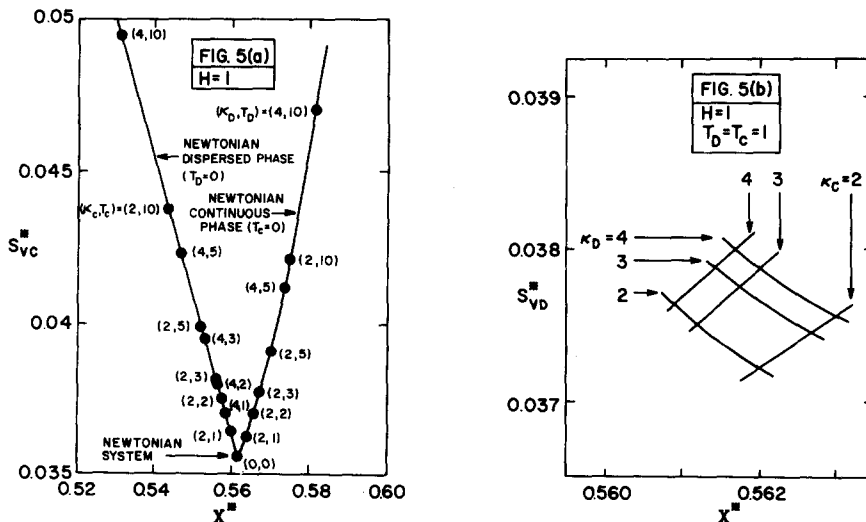


Figure 5. Effects of parameters κ_D and κ_C on critical growth rate and wave number results.

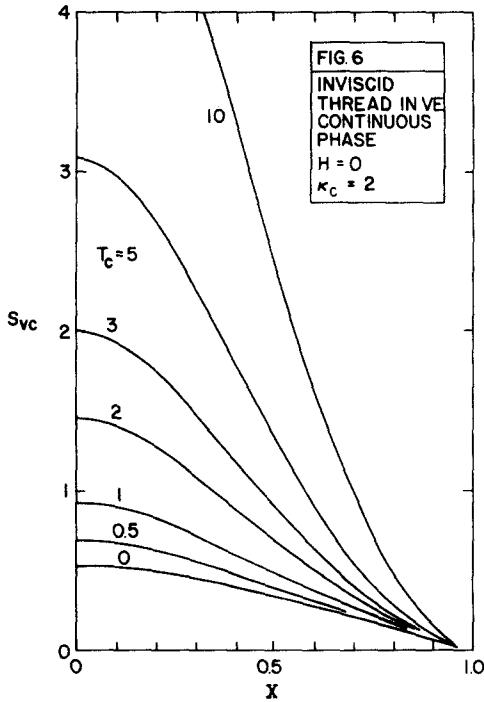


Figure 6.

Figure 6. Results for inviscid thread in a viscoelastic continuous phase.

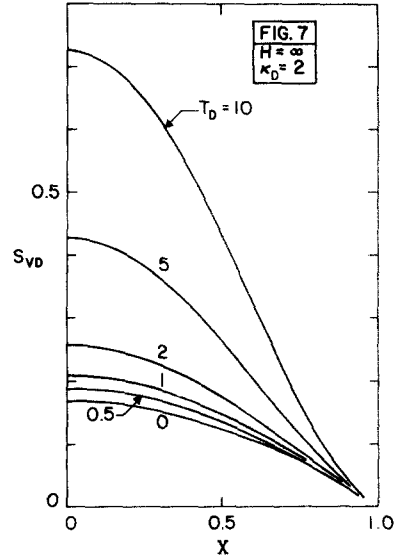


Figure 7.

Figure 7. Results for a viscoelastic thread in an inviscid continuous phase.

At low rotation speeds, the drop is deformed from its original spherical shape to that of a prolate spheroid by the external viscous (and elastic) forces acting on the interface. The major axis of the deformed drop coincides with the x -axis and the minor axis with the y -axis. As the rotation speeds of the cylinders are slowly increased, the drop becomes more and more extended, until at some point, the drop becomes unstable and continuously extends into a long fluid thread. Although the critical conditions for the initiation of this drop “breakup” process is of extreme importance in multiphase mixing and dispersion analyses (see Flumerfelt 1969, Lee 1972, Tavgaç 1972, Yu 1974), the interest here is in the instabilities associated with the second breakup process, i.e. the breakup of the long threads into fine droplets. To achieve the latter in the four roller apparatus under stationary conditions, a drop breakup experiment is conducted to the point where a long fluid thread is obtained, at which time, the rotation of the rollers is stopped and the breakup of the suspended fluid thread is observed. Nearly stationary (or quasi-stationary) conditions are possible in such experiments if the fluids involved are

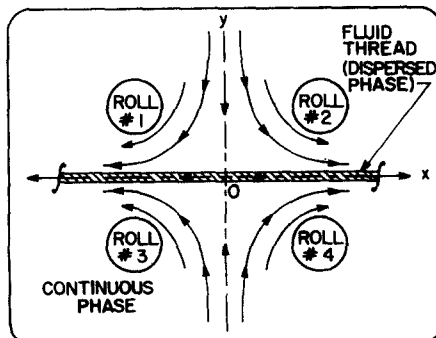


Figure 8. Schematic diagram of four-roller apparatus.

sufficiently viscous, which was the case in the work here. Such an experimental approach has also been used by Rumscheidt & Mason (1962) in studies of stationary and extending thread instabilities. (The breakup characteristics of deformed droplets and extending fluid threads will be considered by the current authors in later publications.)

In the studies here, we are interested in both the general qualitative characteristics of the thread breakup process as well as the quantitative measures of critical growth rates and critical wave numbers. In obtaining this information both still and movie photography was used with a Wild M-7 microscope system.

In the Newtonian fluid tests, the continuous phase fluids were silicone oils of various viscosities, and the dispersed phases were different syrup, molasses, and glycerol-water solutions. In the viscoelastic tests, various aqueous polymer solutions (polyacrylamide solutions) were used as the dispersed phase, with the continuous phase being a silicone fluid. The properties of these fluids are given in table 1.

In all Newtonian systems studied, the breakup pattern was quite regular with the thread exhibiting a uniform varicosity of increasing amplitude as the breakup process proceeds (refer to sequences shown in figure 9). Once breakup is achieved, the major drops formed are of nearly uniform size. Between each pair of major drops there is a small satellite drop, and between this first generation satellite drop and the major drop there is an even smaller second generation satellite drop. This trend was observed as far down as our optical resolution allowed.

The measured critical wavenumbers X^* (dimensionless) are shown in figure 10 as functions of the viscosity ratio. For comparison, we also show the predicted results from Tomotika's theory for systems with $Oh_C = Oh_D = 0$. (In the experiments, the calculated values of Oh_C and

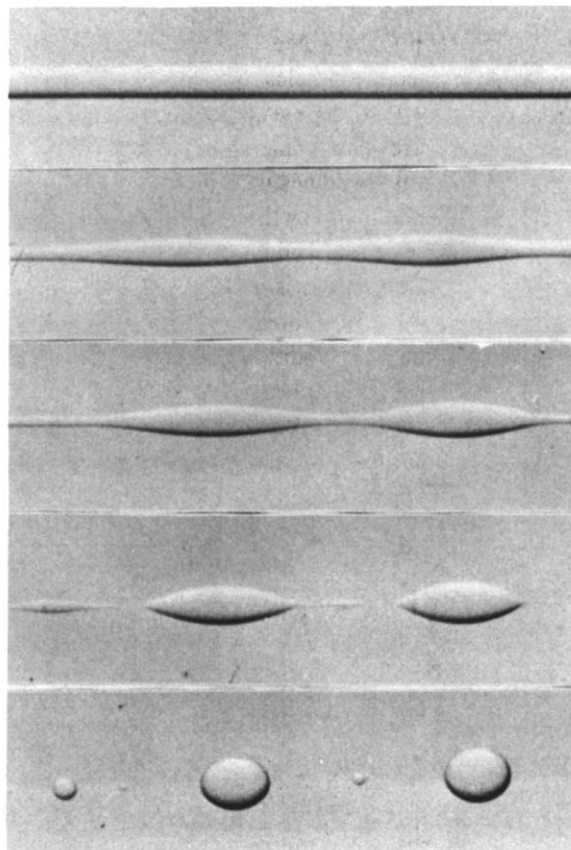


Figure 9. Thread breakup sequence. Newtonian thread (glycerol, $\eta_D = 0.26 \text{ Pa} \cdot \text{s}$) in Newtonian continuous phase (silicone oil, $\eta_C = 30 \text{ Pa} \cdot \text{s}$). Initial thread diameter = 0.0127 cm.

Table I. Properties of fluid systems

(1) Continuous Phase:		Silicone Oil						
		$\eta_c = 30.0 \text{ Pa}\cdot\text{s}$, $\rho_c = 1000 \text{ kg/m}^3$						
(a) Newtonian Threads	ρ_D (kg/m^3)	η_D ($\text{Pa}\cdot\text{s}$)	σ (mN/m)	$H = \eta_D / \eta_c$	λ (sec)	σ (mN/m)	$H = \eta_{OD} / \eta_c$	
Molasses	1450	283.0	26.8	9.42				
Molasses	1440	38.2	28.4	1.27				
Molasses	1430	23.2	28.5	0.77				
Molasses	1410	7.28	26.5	0.24				
Molasses	1390	3.07	26.0	0.10				
Glycerol	1240	0.259	20.6	0.0086				
(b) Viscoelastic Threads	ρ_D (kg/m^3)	η_{OD} ($\text{Pa}\cdot\text{s}$)	κ	λ (sec)	σ (mN/m)	$H = \eta_{OD} / \eta_c$		
2% Polyacrylamide* (DOW Separan AP30)	1066	336.0	3.04	49.5	18.5	11.2		
1.5% Polyacrylamide* (DOW Separan AP30)	1058	101.0	2.68	35.5	22.5	3.4		
1.0% Polyacrylamide* (DOW Separan AP30)	1056	38.1	2.56	21.0	25.0	1.27		
0.75% Polyacrylamide* (DOW Separan AP30)	1056	15.9	2.48	11.1	26.0	0.53		
*In 80-20 Water Glycerine Solution								
(2) Continuous Phase:		Silicone Oil						
		$\eta_c = 30.8 \text{ Pa}\cdot\text{s}$, $\rho_c = 972 \text{ kg/m}^3$						

<u>Newtonian Threads</u>		ρ_D (kg/m ³)	η_D (Pa.s)	σ (mN/M)	$H=\eta_D/\eta_C$
Molasses	1450	283.0	37.5	9.19	
Molasses	1440	35.3	32.0	1.15	
Molasses	1430	23.2	34.6	0.753	
Molasses	1420	11.8	32.8	0.383	
Molasses	1410	7.28	34.1	0.236	
Molasses	1420	6.91	34.2	0.224	
Molasses	1420	5.67	32.6	0.184	
Molasses	1400	4.25	35.6	0.138	
Molasses	1390	3.07	38.0	0.0997	
Molasses	1380	2.88	37.3	0.0935	

<u>Viscoelastic Threads</u>		ρ_D (kg/m ³)	η_{OD} (Pa.s)	κ	λ (sec)	σ (mN/m)	$H=\eta_{OD}/\eta_C$
1.5% Polyacrylamide* (DOW Separan AP30)	1150	325.0	3.27	26.8	16.9	3.16	
1.5% Polyacrylamide** (DOW Separan AP30)	1060	170.0	3.24	20.1	9.3	16.5	
1.0% Polyacrylamide** (DOW Separan AP30)	1050	26.7	2.78	10.4	15.9	2.59	
0.85% Polyacrylamide** (DOW Separan AP30)	1050	24.5	2.72	11.1	15.2	2.38	
0.75% Polyacrylamide** (DOW Separan AP30)	1050	19.8	2.87	7.86	17.0	1.92	
0.5% Polyacrylamide** (DOW Separan AP30)	1040	5.35	2.51	5.52	19.2	0.519	

(3) Continuous Phase: Silicone Oil
 $\eta_C = 10.3 \text{ Pa.s}$, $\rho_C = 972 \text{ kg/m}^3$

* In 50-50 Water-Glycerine Solution
 ** In 80-20 Water-Glycerine Solution

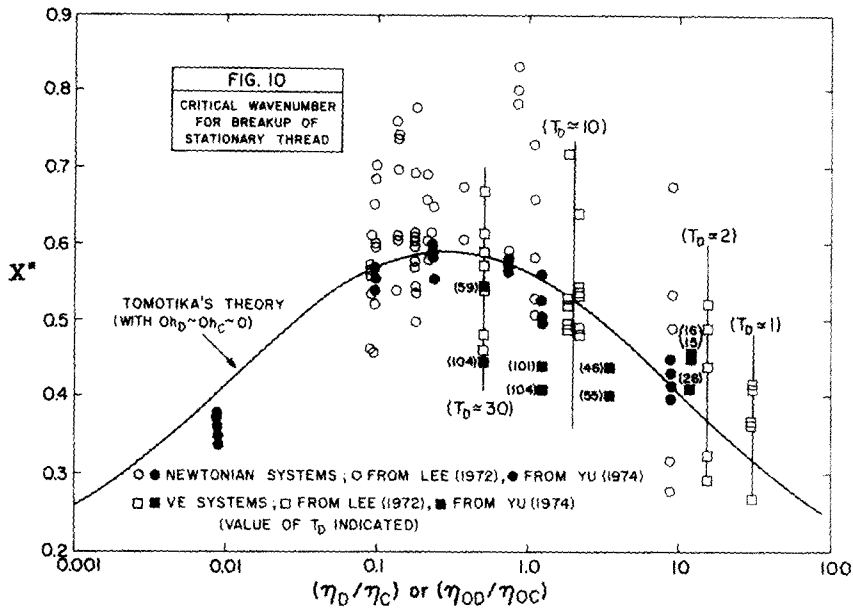


Figure 10. Comparison of linearized theory with experimental results—Newtonian and viscoelastic threads.

Oh_D were small, on the order of 0.01 or less.) Although the data are scattered, the experimental results are in general agreement with the theoretical predictions.

Critical wavenumber data were also obtained for the polymer solutions listed in table 1. These are also plotted in figure 10. In each case the viscosity ratio was taken as the ratio of the zero-shear viscosities. All of the data correspond to small Oh_C and Oh_D conditions, however, the elasticity number, T_D , varies from case to case due to the different material properties and the different initial thread diameters used in the tests. The particular value of T_D associated with each viscoelastic thread data point (or set of data points) is indicated directly on the figure.

In general, the critical wavenumber results are also in rough agreement with the theoretical predictions of the linearized theory. In particular, figure 4 indicates that T_D should have little effect on X^* at $H \equiv \eta_{0D}/\eta_{0C} > 1$. Although the data in figure 10 are too scattered to verify this, the general trend of the results (X^* vs H) are in agreement with figure 4.

It is interesting to note that systems with high viscosity ratios always take longer time periods before unstable varicosities are observed on the thread (as opposed to short time periods for low viscosity ratios systems). With the relatively high viscosity systems used here, and particularly for those systems where $H > 1$, the threads were found to maintain their cylindrical shapes for long periods after the flow had been stopped. In some cases, time periods on the order of 1 min or more were required before the occurrence of varicosities on the interface of the thread.

Clearly, this significant reduction in varicosity growth rate stems largely from the viscous damping effects of the high viscosity thread. In addition, if the thread is sufficiently small, and surface active agents are present, significant dynamic interfacial effects (dynamic interfacial tension, interfacial tension gradients, and interfacial viscosities) could arise which could also contribute to the retardation of varicosity growth kinetics. It is thought that such effects may account for the large scatter of the data in figure 10. In particular, from experiment to experiment the thread interface may be at different stages of equilibrium with respect to surfactant adsorption-desorption processes between the interface and the surroundings. Threads which had initially been stretched out at rapid extension rates would initially have lower surface concentrations of surfactant and therefore high interfacial tensions. Also, large diameter threads would tend to equilibrate slower than small diameter

ones. In light of such possibilities, it is not surprising that accurate reproducibility of X^* data is difficult.

Even though the variance of X^* data is rather large, it is somewhat striking that the threads break uniformly with regular wave patterns and drop sizes. The nature of the waves (refer to figure 9) and the general agreement with Tomotika's theory (figure 10) indicate that linearized stability theory has a degree of validity in this problem.

In order to experimentally compare the relative instability between Newtonian threads and viscoelastic threads, the amplitude of the varicosity, ξ , at various times *before* breakup was measured on two individual systems with the same viscosity ratios, one for a Newtonian system, and one for a viscoelastic system. The fluid systems are indicated on figure 11. The results are presented on a semilogarithm scale with ξ/a_0 plotted vs time. Here $\xi/a_0 = 1$ corresponds to the breakup point and t' corresponds to the time before the breakup point. The comparison here shows that the viscoelastic thread is less stable than the Newtonian thread (with higher slope) except possibly for a short period before the breakup point. The almost linear relation for the Newtonian thread agrees with Tomotika's linear stability theory.

In most experiments the breakup patterns for the viscoelastic systems were fairly uniform with evenly spaced drops eventually being formed. The observed varicosities on the viscoelastic threads were somewhat different from those observed with Newtonian systems. In particular, a bead-thread-bead pattern was more evident with the viscoelastic systems (see figure 12). The appearance of beads is similar to what is observed with jets, however in the latter cases, they do not tend to be as uniformly spaced as observed here.

In some cases, irregular breakup patterns were observed with the polymeric systems. These were generally observed with larger diameter threads and in the latter stages of the thread breakup process. Such irregular patterns might be due to some external mechanical vibration in the apparatus or to other physical effects (surface tension gradients resulting from surface contaminants; inertial effects; non-linear rheological effects, etc.)

Finally, we should mention that the measured ratio of diameters of the final main droplets and that of the thread (initially) is fairly uniform for all of the different types of systems tested; this ratio taking on values between 2.0 and 2.6. Of course, this simply reflects the small effects of the elasticity number and viscosity ratio on X^* for the ranges covered by the experiments and test fluids.

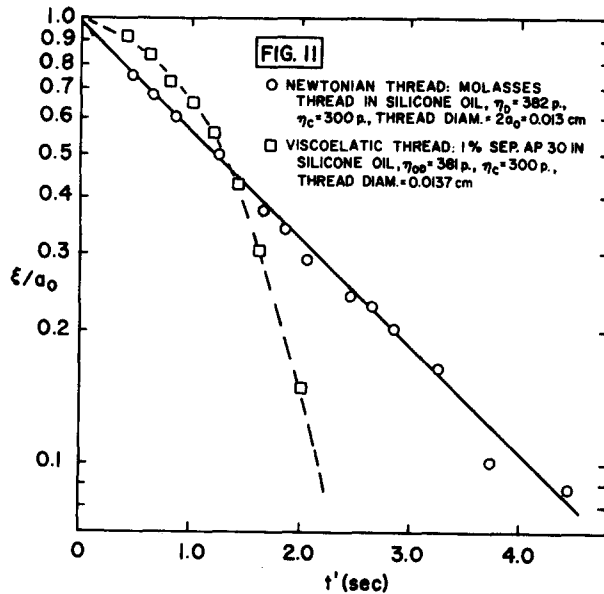


Figure 11. Experimental comparison of wave amplitude versus time for Newtonian and viscoelastic threads, each with similar viscosities and initial thread diameters. Note: t' is time to breakup; i.e. $t' = 0$ corresponds to breakup.

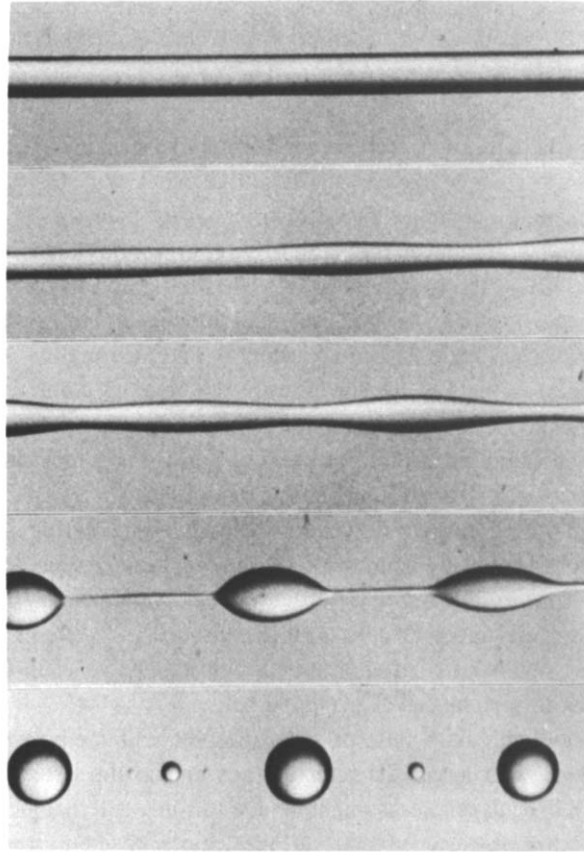


Figure 12. Thread breakup sequence. Viscoelastic thread (0.75 per cent polyacrylamide in 80–20 water-glycerine solution, $\eta_{OD} = 15.9 \text{ Pa} \cdot \text{s}$) in Newtonian continuous phase (silicone oil, $\eta_C = 30 \text{ Pa} \cdot \text{s}$). Initial thread diameter $\approx 0.0176 \text{ cm}$.

CONCLUDING REMARKS

The results obtained here clearly support the observations of other investigators that viscoelastic cylindrical fluid bodies are less stable than corresponding Newtonian systems, both with comparable viscous properties. However, observations here are somewhat more definitive since close approximations to true stationary thread breakup experiments were possible with tests in the four-roller device. Such experiments are certainly more desirable than jet breakup tests in studies of stationary and uniformly moving thread instabilities. Based upon the regular breakup patterns observed here (in most cases) and general agreement of the results with the linearized theory predictions, it would appear that the irregularities observed with viscoelastic jets, i.e. irregular bead-thread patterns, arise from effects other than those neglected in the linearized theory analysis. In particular, one must observe that jet breakup experiments, particularly for viscoelastic fluids, are only crude representations of true stationary or uniformly moving flow conditions in the thread. Obviously, if the fluids have sufficiently large characteristic times, the stresses built up in the nozzle region can affect the instability behavior over significantly large distances along the thread. Such stress relaxation effects are not included in analyses of stationary and uniformly moving threads like that presented here. Obviously, deviations between observations and predictions must occur when such effects are neglected.

In general, the observations presented here support the validity of the linearized theory for describing stationary thread instability precesses. This is not surprising since the base flow in this case is zero motion. Other relatively successful applications of linearized theory, such as the predictions associated with the problem of a fluid layer heated from below, also have this

zero base flow characteristic. In the problem here, the apparent validity of the linear theory gives credence to the theoretical results of the present paper as well as those given in Part I and provides a basis for predicting breakup phenomena under conditions not always easily achieved in the laboratory.

NOMENCLATURE

- a diameter of an undisturbed cylindrical thread, m
 $i = \sqrt{-1}$
 k wavenumber, m^{-1}
 p hydrostatic pressure, Pa
 q a dummy number used in [6]–[14]
 s a time parameter, $(= t - t')(s)$,
 t time, s
 t' previous time, (the superscript, is not a representation for derivative), s
 \underline{u} velocity vector, $= (u_r, u_\phi, u_z)$, m/s
 x the extensional axis in the flow field of a four-roller apparatus
 y the compressive axis in the flow field of a four-roller apparatus
 G density ratio, $(= \rho_D/\rho_C)$
 H ratio of the zero-shear viscosities, $(= \eta_{0D}/\eta_{0C})$
 Oh Ohnesorge numbers, $(= (a\sigma\rho)^{1/2}/\eta)$
 $Re\{\}$ the real part of $\{\}$
 S dimensionless growth-rate, $(= a\alpha\eta_0/\sigma$ in the systems considered in Part II)
 T elasticity number, $(= \sigma\Lambda/2a\eta_0)$
 U viscosity ratio, $(= \eta_D/\eta_C)$
 X dimensionless wavelength, $(= ka)$
 $Z()$ the Riemann-zeta function

Greek letters

- α growth rate, s^{-1}
 $\dot{\gamma}$ strain rate, s^{-1}
 ∇ gradient operator (defined in [1] of Part I)
 $\delta(t)$ the Dirac delta function
 ϵ a frequency parameter defined in [10], $(= i\omega)$
 η viscosity, $Pa \cdot s$
 η_0 zero-shear viscosity, $Pa \cdot s$
 κ a slope parameter for the power-law region
 Λ characteristic time, s
 ξ amplitude of the varicosity on an unstable thread, m
 ρ density, kg/m^3
 σ interfacial tension, $Pa \cdot m$
 τ stress, Pa
 Φ a memory function
 Ψ a function defined in [12]
 ψ Stokes' stream function, m^3/s
 ω frequency of an oscillation

Superscripts

- $\bar{}$ the one-sided Laplace transform of a quantity
 $\hat{}$ the two-sided Laplace transform of a quantity
 $*$ a complex quantity (except for S^* and X^* which correspond to critical growth rate and wavelength quantities)

Subscripts

- C* continuous phase
D dispersed phase
r radial-component quantity in a cylindrical coordinate system
V a quantity relating to viscous effects
z axial-component quantity in a cylindrical coordinate system
ϕ polar-component quantity in a cylindrical coordinate system

REFERENCES

- BIRD, R. B., ARMSTRONG, R. C. & HASSAGER, O. 1977 *Dynamics of Polymeric Liquids*. Wiley, New York.
- FLUMERFELT, R. W. 1972 Drop breakup in simple shear fields of viscoelastic fluids. *Ind. Engng Chem. Fund.* **11** 312–318.
- GOLDEN, M., YERUSHALMI, J., PFEFFER, R. & SHINNAR, R. 1969 Breakup of a laminar capillary jet of a viscoelastic fluid. *J. Fluid Mech.* **38**, 689–711.
- GOLDEN, M., PFEFFER, R. & SHINNER, R. 1972 Breakup of capillary jet of a non-Newtonian fluid having a yield stress. *Chem. Engng J.* **4**, 8–20.
- HUPPLER, J. D., ASHARE, E. & HOLMES, L. A. 1967 Rheological properties of three solutions—I. Non-Newtonian viscosity, normal stresses, and complex viscosity. *Trans. Soc. Rheol.* **11**, 159–179.
- KROSSER, F. W. & MIDDLEMAN, S. 1969 Viscoelastic jet stability. *AIChE J.* **15**, 383–386.
- LEE, W. K. 1972 Deformation and breakup of liquid drops and threads in extensional flow fields. Ph.D. Dissertation, Univ. of Houston.
- MIDDLEMAN, S. 1965 Stability of a viscoelastic jet. *Chem. Engng Sci.* **20**, 1037–1040.
- RUMSCHEIDT, R. D. & MASON, S. G. 1962 Breakup of stationary liquid threads. *J. Coll. Sci.* **17**, 260–269.
- SPRIGGS, T. W. 1965 A four-constant model for viscoelastic fluids. *Chem. Engng Sci.* **20**, 931–940.
- TAVGAC, T. 1972 Drop deformation and breakup in simple shear fields. Ph.D. Dissertation, Univ. of Houston.
- TAYLOR, G. E. 1934 The formation of emulsions in definable fields of flow. *Proc. R. Soc. London* **A146**, 501–523.
- YU, K. L. 1974 The deformation and breakup of liquid drops in an extensional flow field, and the instability of stationary and extending threads. M. S. Thesis, Univ. of Houston.